

## RESEARCH

## Removing of Hardness Solids from Groundwater by Thermogenic Synthesis Zeolite

DOI: 10.15436/JESES.1.3.5

Abd El Hay Ali Farrag<sup>1</sup>, Th. Abdel Moghny<sup>2</sup>, Atef Mohamed Gad<sup>1,3</sup>, Saleem Sayed Saleem<sup>3</sup>, Mahmoud Fathy<sup>2</sup>, Muhamed Atef Ahmed<sup>3</sup>

<sup>1</sup>Assiut university faculty of science geology department, Box. No. 71516, Assiut, Egypt

<sup>2</sup>Applications Department, Egyptian Petroleum Research Institute (EPRI), 1 Ahmed El-Zomer, Nasr City, Box. No. 11727, Cairo, Egypt

<sup>3</sup>Assiut and new valley company for water and waste water fax No: 088229347

RECEIVED DATE: 23-11-2016; ACCEPTED DATE: 08-12-2016; PUBLISHED DATE: 28-12-2016

CORRESPONDENCE AUTHORS: Atef Mohamed Gad

E-MAIL: atefgad98@yahoo.com

## CONFLICTS OF INTEREST

THERE ARE NO CONFLICTS OF INTEREST FOR ANY OF THE AUTHORS.

## ABSTRACT:

Calcium and magnesium hardness solids in groundwater are very common and caused major problems for drinking and household purposes. This study aims to synthesize zeolite-4A from kaolinite for removing the total hardness ions from Assiut Governorate groundwater wells in Egypt. The kaolin was hydrothermally calcinated through metakaolinization and zeolitization processes to produce crystalline zeolite-4A. The chemical composition and morphology of crystalline zeolite-4A was characterized by using X-ray diffraction (XRD) and scanning electron microscopy (SEM). Then the column experiments were conducted to study the performance of crystalline salt-4A as ion exchange and investigate their operation parameters and regeneration conditions. Thomas and Yoon-Nelson models were applied to predict the adsorption capacity and time required for 50% breakthrough curves. The effects of initial concentrations of 550 mg/l for total  $\text{Ca}^{+2}$  and  $\text{Mg}^{+2}$  hardness, feed flow rate of 10-30 ml/min, and height range of 1.0–4.0 cm on the breakthrough behavior of the adsorption system were studied. The obtained results indicated that the synthesized zeolite-4A can remove total hardness ( $\text{Ca}^{+2} + \text{Mg}^{+2}$ ) ions from groundwater to the permissible limit according to the standards drinking water law.

**KEYWORDS:** groundwater, water hardness, Egyptian kaolin, synthetic zeolite, metakaolinization, zeolitization.

## INTRODUCTION

Groundwater as an essential source of fresh water used for drinking, household, agriculture, industry after rivers and rain in most parts of the world. But many components involved in groundwater affecting taste and quality. Total hardness and calcium hardness solids are common components affecting negatively on the taste and quality of the drinking water, especially in the locations near rivers or channels, which doesn't recharge from the aquifer of limestone or clays (Ben Abda, Schäfer et al. 2015). For this reason, soils are one of the most important natural filter for the water by far in agricultural and forest soils (Brevik et al., 2015; Keesstra et al., 2012; Keesstra, 2007). For instance, soil erosion

(Rodrigo Comino et al., 2016a, 2016b) or soil pollutants (Novara et al., 2016, 2013) must be controlled.

Water hardness are due to calcium and magnesium cations, and can be reduced by several methods such as electrode ionization process, electro membrane processes, capacitive deionization, fluidized pellet reactor, and reverse osmosis membrane (Chen, Zhang et al. 2012). Reverse osmosis treatment is a useful method to avoid these hardness solids, but it's not satisfactory due to several reasons: i) it's slow and produce more waste water; ii) a few amount of potable water is produced in a long time; iii) consumes great electricity energy support; and, iv) requires highly convenient technicians for the operation process and

loses large amount of raw water as a waste within the production process. In addition, less one gallon of potable water is produced within more than six hours, as well as, seven to eight gallons of waste water are generated in that time (Mahmoud Fathy 2016).

Finally, it's required a high pressure associated with high electrical energy costs to operate the unit. For those reasons, the authors (citation) suggest to use ion exchange process based on synthetic zeolite as filtration media for adsorption of hardness solids, because it is low cost sorbents and that process can be consider one of the promising techniques. The mechanism of synthetic zeolites as ion exchange depends on use their granular negative charge to exchange ions present in their structure with ions present in the water, thereby, it can produced a very large amount of treated water through a short time, and it's very easy regeneration by passing 10% NaCl solution through it (Calvo, Canoira et al. 2009, Cai, Turner et al. 2015).

This study aimed to apply zeolite synthesized from Egyptian kaolin as ion exchanger to remove excess total and calcium hardness ions in groundwater wells of Assiut Governorate, according to WHO (2004) and the standards Egyptian drinking water Law No. (458/2007). In this respect, columns experiments of synthesized zeolite-4A were conducted to study their performance as ion exchange and investigate their operation parameters and regeneration conditions.

## 2. Experimental Study

### 2.1. Materials

Groundwater samples were taken from about 850 plots producing drinking water, covering all Assiut Governorate during 2010-2015 and to identify the most contaminated wells with about 40 % of total hardness and Calcium hardness ions. The filtration media mainly consisted of zeolite-4A with grain size <0.8 mm that synthesized from natural kaolin that available in south-east Abu zenima in Sinai region-Egypt.

Finally, sandstone has diameter ranged from (0.5 mm to 1.2 mm) was used as filter in the packed column.

### Methods and procedures

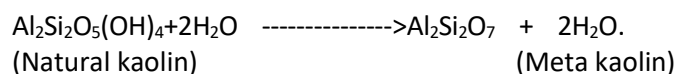
#### 2.2.1 Preparation of Zeolite 4A

Zeolite-4A was synthesized based on Abu zenima kaolin through a) metakaolinization (calcinations or thermal treatment), and (b) zeolitization step (alkaline treatment).

#### a) Calcination or thermal treatment

Natural occurring kaolin was crushed and sieved to the grain size < 80 micron, then expose to high

temperature (greater than 800 °C at approximately 4 hour) to convert kaolin to metakaolin (calcinated kaolin) (Bhatia, Abdullah et al. 2009). The heating process drives off water from the main constituent of kaolin clay mineral ( $\text{Al}_2\text{Si}_2\text{O}_5(\text{OH})_4$ ), and collapses the material structure by producing an amorphous aluminosilicate ( $\text{Al}_2\text{Si}_2\text{O}_7$ ), metakaolin. The process is known as dehydroxylation, hence, both the surface and chemical combined water are removed, rendering kaolin non-plastic and presented by the following equation,



#### b) Zeolitization (alkaline treatment)

This process was achieved by mixed of metakaolin powder with 3M sodium hydroxide solution at ratio of 1: 5 (solid: liquid) with 4 hours stirring at temperature of 100 °C. After that the mixture was filtered, washed with distilled water to remove the excess alkali, decanted and filtered several times till pH 10, then dried at 90°C overnight and crushed to particle size <80 micron. Finally the product was characterized by XRD and ESM examinations (Devrim and Albostan, Guo, Zeng et al. 2013).

#### c) Column Study

Three PVC filter columns having 5 cm inner diameter and 12 cm height were setups and packed with mixing ratio of 1: 1 of <0.8mm synthetic zeolite and 0.5-1.2 mm sand. Three filtration media of 30, 60, and 120-gm weight (that represented bed heights of 1.0 cm, 2.0 cm, and 4.0 cm, respectively), were packed in P.V.C columns at three adjusted filtration rate of 10, 20, and 30 ml / min, respectively. The concentration of total and calcium hardness, of water samples, was analyzed before and after the treatment by selected sequentially every 100 mL of filtered water for analysis according to standard test methods. After filtration, the ion concentrations in the aqueous phase were measured using spectrophotometer model HACH DR6000 (Grande and Rodrigues 2004).

## 3. Results and Discussion

### 3.1. XRD analysis

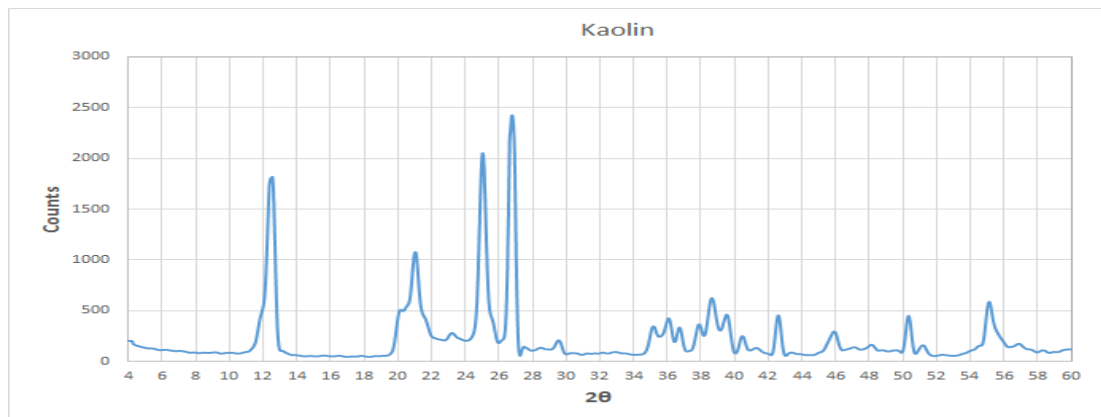
The XRD pattern of hexagonal kaolin mineral sheets before calcination or any treatment shows that the hydroxysodalite having several common peaks located at 13.96, 19.98°, 24.42°, and 35.00° as shown in Figure 1 (El Tahlawi, Farrag et al. 2008, Mustafa and Zaiter 2011). The XRD spectra analysis of hexagonal kaolin was very difficult because kaolin contained several

mineral phases and many impurities. This led to appear of overlapping peaks due to complex structure of hexagonal kaolin. Therefore, additional treatments will be used to remove some ambiguity (Abd El Hay Ali Farrag 2016). At low diffraction angles, there was a fairly large continuous background because of Lorentz polarization and the presence of amorphous phases. Two broad peaks (the first one between  $19^\circ$  and  $33^\circ$  and the second one between  $34^\circ$  and  $43^\circ$ ) were also observed. Furthermore, the low intensity and the more or less pronounced symmetry of the peaks at the smallest angles were likely as a result of the greater disorder of the structure of this kaolin (Mustafa and Zaiter 2011).

Figure 2 presents the XRD pattern of complete poorly crystalline metakaolin formed by calcination of kaolin (at  $800^\circ\text{C}$  for 4 hours), indicating on the formation of a new phase of dehydroxylated, hence the internal structure was destroyed with containing negative charges and shows only one characteristic diffraction peaks located at peaks located at  $19.75^\circ$ , that is

attributed to kaolinite remains in the calcined kaolin. The contents of orthoclase and muscovite are also reduced according to diffraction peak strength, but the content of quartz is still high, so quartz seems inert during calcination. Nepheline ( $\text{NaAlSiO}_4$ ) and little amount of anhydrous sodium aluminosilicate  $\text{Na}_2(\text{Al}_2\text{Si}_3\text{O}_{10})$  are found in the treated kaolin, in addition to disappearing of peaks related to all raw minerals (Guo, Zeng et al. 2013, Luukkonen, Runtti et al. 2016).

Finally, the XRD pattern in Figure 3 illustrated the agglomerated cubic crystals of final synthesized zeolite 4A after treated with  $\text{NaOH}$  solution at  $100^\circ\text{C}$  for 4 hours, and exhibit characteristic peaks at  $2\theta$  values of  $7.2^\circ$ ,  $10.3^\circ$ ,  $12.6^\circ$ ,  $16.2^\circ$ ,  $21.8^\circ$ ,  $24^\circ$ ,  $26.2^\circ$ ,  $27.2^\circ$ ,  $30^\circ$ ,  $30.9^\circ$ ,  $31.1^\circ$ ,  $32.6^\circ$ ,  $33.4^\circ$  and  $34.3^\circ$  its typically matches XRD pattern of zeolite 4A that synthesized at 3 M  $\text{NaOH}$  concentrations by (Abd El Hay Ali Farrag 2016) and found that the synthetic zeolites 4A have more crystalline  $\text{SiO}_2$  in the form of quartz tetrahedral crystal lattices structures (Han, Zou et al. 2009).



**Figure(1).**XRD of Kaolin mineral before calcination or any treatment.

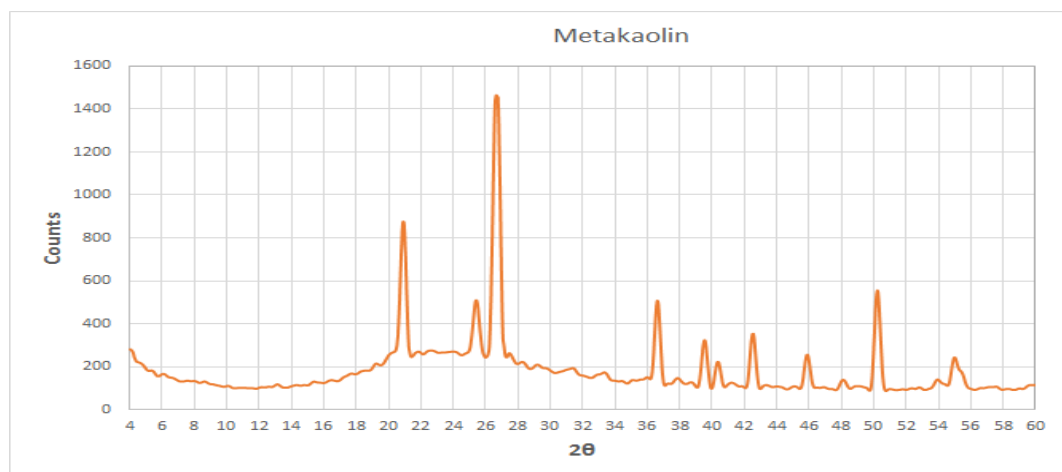


**Figure (2).**XRD of kaolin after calcination at  $850^\circ\text{C}$  for 4 hours.

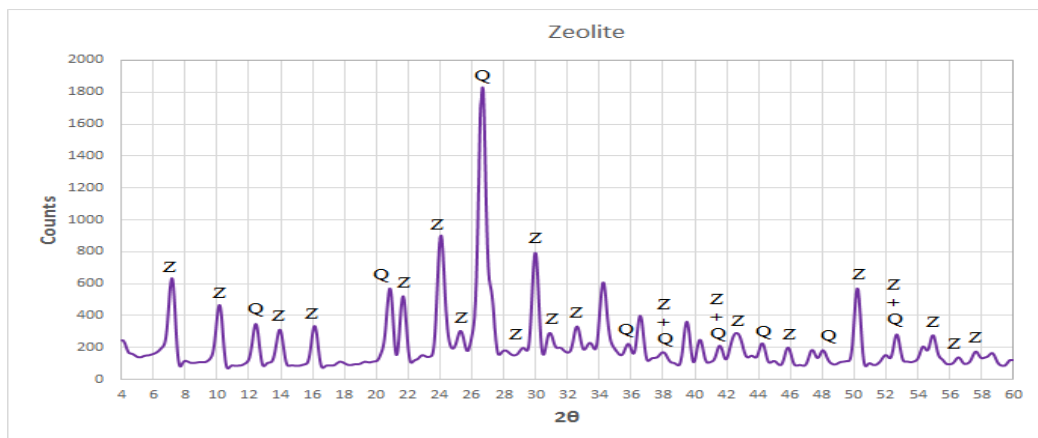
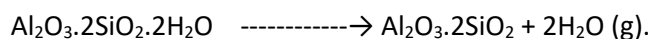


**Figure (3).** XRD of finally synthesized Zeolite 4A after treated with NaOH solution at 100 °C during 4 hours

### 3.2. Scanning Electron Microscope SEM analysis

It is known that the framework structure of zeolite is described as a combination of two inter connected channel systems. SEM micrographs of kaolinite prior to treatment, after calcination and the final synthesized zeolite-4A, are shown in Figures (4a, 4b, 4c).

Figure 4a represents SEM images of kaolin powders at different particle sizes. As can be observed, the kaolin particles at both particle sizes show crystallinity flake-like structure. This is because that powder has a random structure that induces different shapes and sizes and could change due to the process preparation. Nevertheless, the particle agglomeration is observed especially for type A kaolin (Fig. 4(a) Hosseini et al., 2014). Figure 4b shows the SEM of kaolin after calcination (metakaolinite) at 800 °C during 4 hours. It was clear that the calcination process increasing all of the whiteness, hardness, improves the electrical properties, and alters the size and shape of the kaolin particles. Calcination process that occurs at 800 °C for the dehydroxylation kaolin indicating on the formation of complete poorly crystalline metakaolin as a new phase of dehydroxylated, hence the internal structure was destroyed with containing negative charges as illustrated in XRD of kaolin after calcination (Figure 2) (Inglezakis and Grigoropoulou 2004). Such process can be describe by the following chemical equations,



During this reaction, as SEM showed, the higher-order reflections lost their intensity and vanished in the SEM background. This result led to the opinion, that the metakaolinite can be amorphous, now a conception of the short-range order crystalline structure of metakaolinite predominates.

As shown from the images in Figure 4c, a marked change took place in the morphology of the starting materials. The cubic crystalline morphology in Figure 4c, typically of the zeolitic products obtained consisting of sinusoidal channels (along ) with a circular cross section interconnected with straight channels (along) of elliptic cross section (5.3 Å × 5.6 Å). The scanning electron micrographs (SEM) of the synthesized zeolite reveals on the presence of slightly different crystals sizes with the same cubic morphology at an average diameter of approximately 4 μm. In addition, this technique reveals on the absence of any amount of amorphous material in the synthesized zeolite, which indicates the presence of zeolite 4A in a high degree of crystallinity. It is known that the framework structure of zeolite is described as a combination of two inter connected channel systems. Also, this methodology advantage by the low cost-effective alternative to produce zeolite 4A (Kazemimoghadam and Mohammadi 2007).

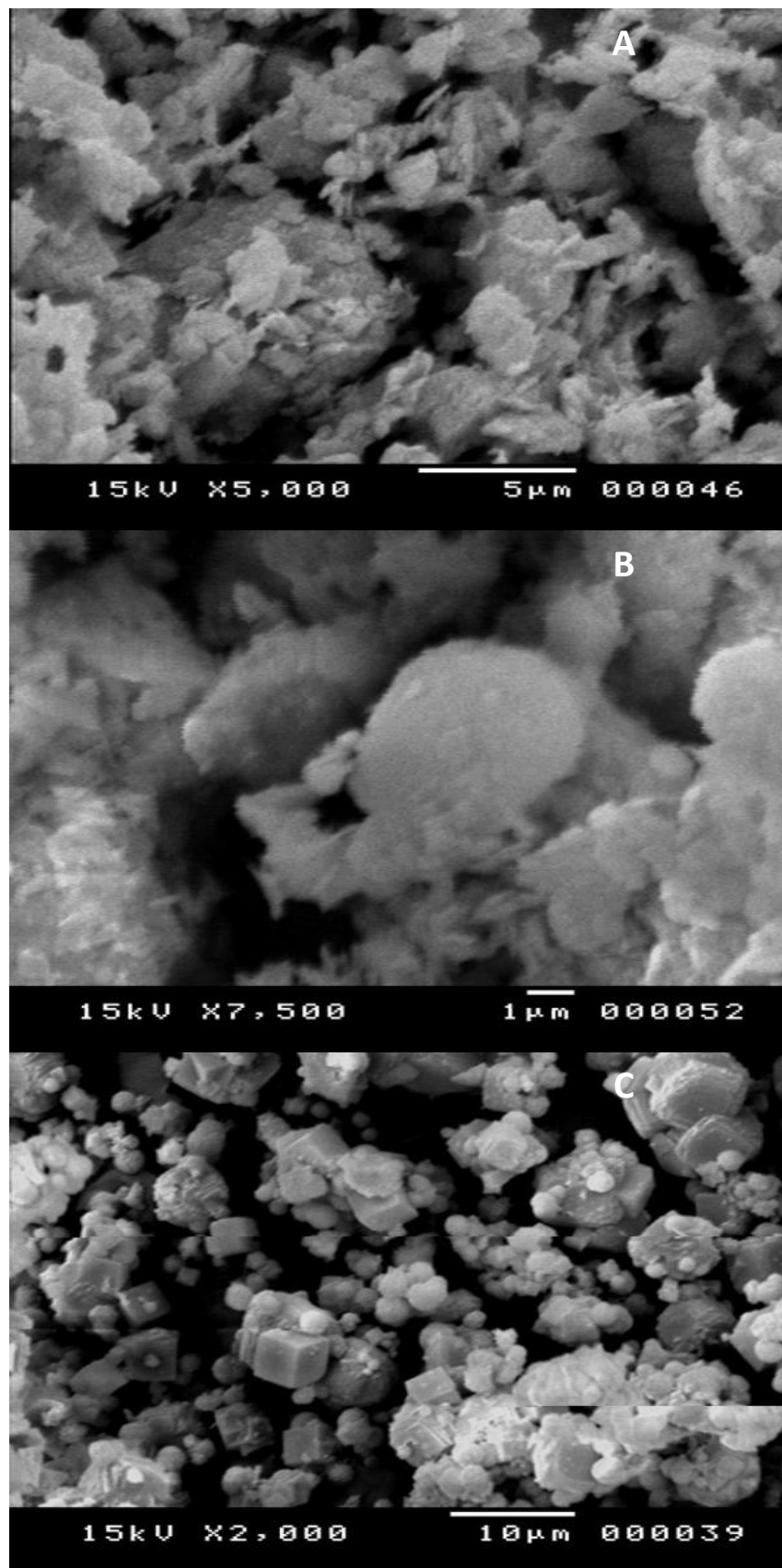


Figure (4).SEM of A) kaolin, B) kaolin after calcination and C) zeolite 4A.

### 3.3. Contact time research

The influence of contact time on adsorption of calcium and total hardness at flow rate of 20ml/min from raw water containing  $550\text{mg}\cdot\text{L}^{-1}$  calcium hardness and  $420\text{mg}\cdot\text{L}^{-1}$  total hardness have been studied, the results are shown in Figure 5. It's found that the initial adsorption was slightly rapid within the first 100 min due to the adsorption of  $\text{Ca}^{+2}$  and total hardness onto the exterior surface. Then the ions enter into interior zeolite-4A (Kazemimoghadam and Mohammadi 2007). After that, the adsorption rate decreased substantially with time till equilibrium position. The adsorption process was attained to equilibrium at 160 and 200 min, as well as, the removal efficiency reached to 35% and 100% for calcium and total hardness, respectively.

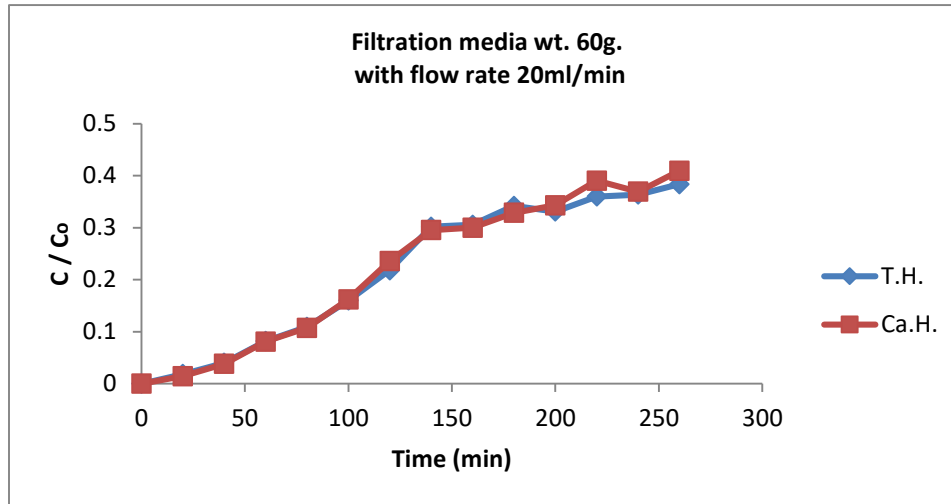


Figure (5). Effect of contact time on the removal of calcium and total hardness at flow rate of 20ml/min.

#### 3.3.1. Effect of flow rate

Flow rate variations another factors influences on the breakthrough. Therefore, the adsorption of 550 mg/l total hardness solids concentrate ions on zeolite media was investigated at varying flow rate of 10, 20 and 30 ml/min and at bed height of 4 cm (120g) as shown in Figure 6. From figure it was observed a significant shrinkage in breakthrough curves as the flow rate increased from 10 to 30 mL/min, this because, an increase in flow rate led to reduce the external film mass resistance over the zeolite4A surface leading to decrease the residence time. Thereby, the decreasing of saturation time leads to dominate the removal efficiency. Conversely, at lower flow rate, the period of mass transfer inside the zeolite-4A pores, would increase and allow more binding accession sites in all cases (calcium and total hardness) (Gupta et al., 2004).

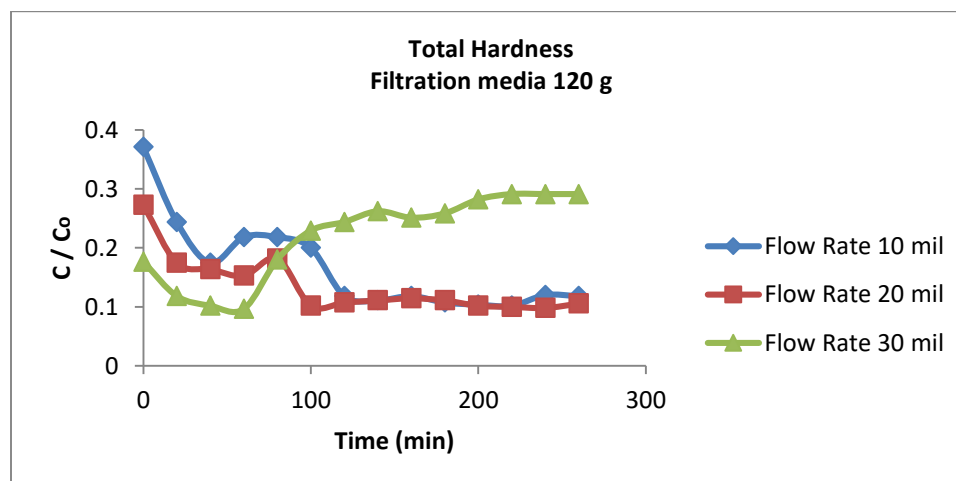
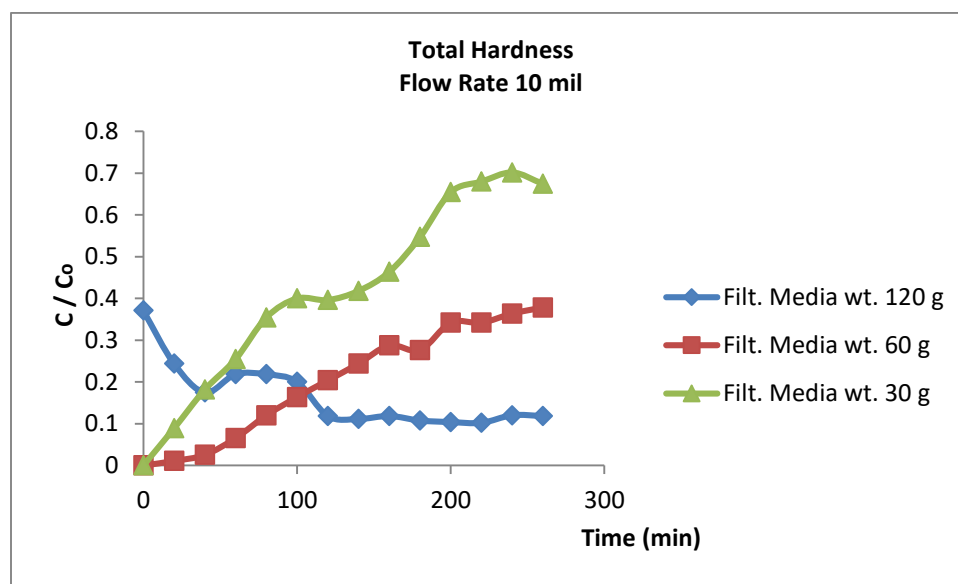


Figure (6). Effect of variation of flow rate on the removal of 550 mg/l Total hardness at constant zeolite height of 4 cm.

### 3.3.2. Effect of bed height

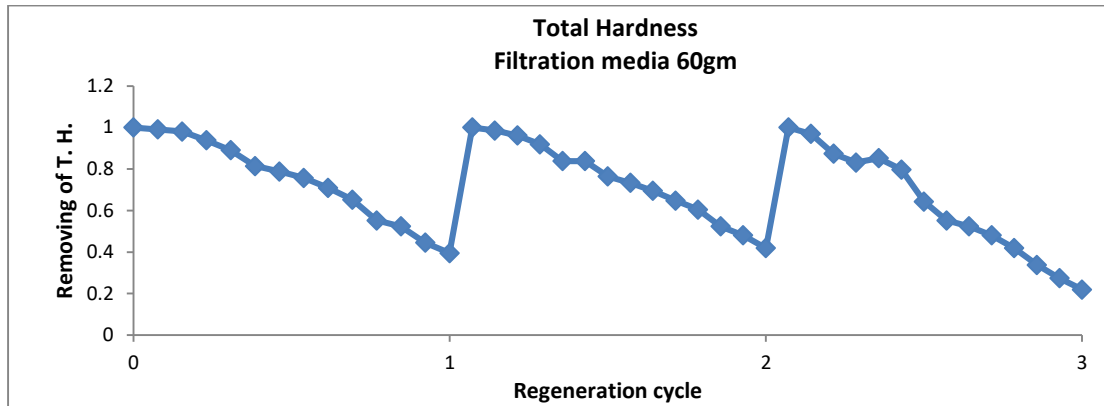
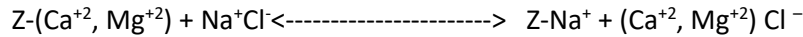
The adsorption of total hardness ( $\text{Ca}^{+2}$ ,  $\text{Mg}^{+2}$ ) ions in the packed column is largely dependent on the bed height, which is directly proportional to the quantity of synthetic zeolite 4A. For this respect, three bed height of 1, 2 and 4 cm were selected for packed column filtration that corresponding of 30 g, 60 g and 120 g synthetic zeolite 4A, respectively. The adsorption breakthrough curves obtained by varying the bed heights at a flow rate of 10 mL/min and at 550 mg/L inlet total hardness ( $\text{Ca}^{+2}$ ,  $\text{Mg}^{+2}$ ) concentrations is presented in Figure 7. It's found that the faster breakthrough curves were observed at bed height of 1 cm, while the slowest breakthrough curve was observed at a bed height of 2 and 4 mm. That is means the bed capacity was increased when the bed height increased from 1 to 4 cm, i.e., higher beds contain more adsorbent; therefore, more binding sites will be available for the total hardness ions ( $\text{Ca}^{+2}$ ,  $\text{Mg}^{+2}$ ) to attach (Mahmoud Fathy 2016), which will eventually lead to the attainment of a higher bed capacity. Additionally, an increased bed height resulted in more contact time being available for the total hardness ions ( $\text{Ca}^{+2}$ ,  $\text{Mg}^{+2}$ ) to interact with the adsorbent (Mahmoud Fathy 1 and 1 2015). This phenomenon has allowed the total hardness ions ( $\text{Ca}^{+2}$ ,  $\text{Mg}^{+2}$ ) to diffuse deeper into the adsorbent. Subsequently, the percentage of total hardness ions removal increased when the bed height was increased (Gupta et al., 2004)



**Figure (7).** Effect of zeolite height variation on the removal of 550 mg/l total hardness at flow rate of 10ml/min. (Filt. Media wt = weight of mixed zeolite and sand used for filtration)

### 3.3.3. Regeneration cycles of zeolite media filtration

Figure 8 illustrates the adsorption/desorption of total hardness for three regeneration cycles. Several regenerated times (more than 3 cycles) were conducted for solution employed 10% NaCl and 550 mg/l total hardness ( $\text{Ca}^{+2}$ ,  $\text{Mg}^{+2}$ ) concentrations to determine the adsorption/desorption capacity of the mineral. In the first run before using NaCl as regeneration, the adsorption capability of zeolite is approximately not exceed than 70% and reach to 100% after using NaCl. The adsorption/desorption capability of zeolite reach to about 100% within the first three regeneration, and the removal efficiency of total hardness reduced to approximately 50%. Finally, the regeneration efficiency reduced as the number of regeneration cycles increased. The decrease in adsorption/desorption with increasing cycles was steeper. One can conclude that at first cycle the adsorbent solutions exhibited the highest desorption performance. It was observed that the adsorption capacity of mineral increased during the first two cycles when using NaCl as desorbing agent because it's enhanced the metal uptake capability of zeolite by replacing mobile ions originally present in the mineral. This finding agrees with previous research work (Abd El Hay Ali Farrag 2016).



Figures (8). Illustrated the adsorption/desorption of total hardness for three regeneration cycles.

### 3.3.4. Breakthrough curves modeling

In order to describe the fixed bed column behavior and scale up for the industrial applications, two models, Thomas, and Yoon-Nelson were conducted to fit the experimental column data (Abanades, Arias et al. 2015). Thomas model is widely used in performance modeling of columns. The arithmetic expression for the model of adsorption column is given in Equation 1 (Gupta, Gaur et al. 2004):

$$\frac{C_t}{C_0} = \frac{1}{1 + \exp\left[\left(\frac{K_{Th}q_e x}{Q}\right) - K_{Th}C_0 t\right]} \quad \text{Equation Eq.1}$$

where  $k_{Th}$  (mL/min.mg) is the Thomas model constant,  $q_e$  (mg/g) is the predicted adsorption capacity,  $x$  is mass of adsorbent (g),  $Q$  is influent flow rate (mL/min),  $C_0$  is initial solution concentration (mg/l), and  $C_t$  is effluent solution concentration (mg/L). The second linear equation of Thomas model is expressed below

$$\ln \frac{C_t}{C_0} - 1 = \left(\frac{K_{Th}q_e x}{Q}\right) - K_{Th}C_0 t \quad \text{Equation Eq.2 (Marcussen 1982)}$$

From the regression coefficient ( $R^2$ ) and other parameters, it can be concluded that the experimental data fitted well with Thomas model. The models parameters are listed in Tables 1 and 2 show that as the flow rate increased, the value of  $k^{th}$  decreased whereas the value of  $q_0$  showed a reverse trend, that is, increased with increasing of the flow rate. Similarly,  $q_0$  values decreased and  $k^{th}$  values increased with increasing the flow rate. Similar trend has also been observed for sorption of total hardness ( $Ca^{+2} + Mg^{+2}$ ) by zeolite-4A. The well-fitting of the experimental data with the Thomas model indicate that the external and internal diffusion will not be the limiting step (Bertoni, Medeot et al. 2015).

Table 1. Values of Thomas model statistical parameter after removal of total hardness ( $Ca^{+2} + Mg^{+2}$ ) by zeolite:

$q$ (mg g <sup>-1</sup> )	R 2	k Th	Flow (mL min <sup>-1</sup> )
1550.395	-0.90151	0.002764309	10
2620.772	-0.89109	-0.001416225	20
-2425.1	0.941445	0.001533116	30

Yoon-Nelson model does not require data about the characteristics of the system including the type of adsorbent as well as the physical properties of the adsorption bed. The Yoon-Nelson equation is expressed as

$$\frac{c_t}{c_0 - c_t} = \exp(K_{YN}t - \tau K_{YN}) \quad \text{Equation Eq.3(M. El-Sayed 2016)}$$

where ( $K_{YN}$ ) is the rate constant ( $\text{min}^{-1}$ ) and ( $\tau$ ) is the time required for 50 % breakthrough (min). The values of the rate constant  $K_{YN}$  increased with the flow rate and the initial concentration (Padilha, Padilha et al. 2015).

The Yoon-Nelson is a linear model for a single component system as expressed by (Abd El Hay Ali Farrag 2016),

$$\ln \frac{c_t}{c_0 - c_t} = K_{YN}t - \tau K_{YN} \quad \text{Equation Eq.4}$$

A model based on the assumption that the rate of decrease in the probability of adsorption of adsorbate molecule and the adsorbate breakthrough on the adsorbent is proportional to the probability of the adsorbate adsorption (Fathy, Moghny et al. 2014).

The values of  $K_{YN}$  and  $\tau$  along with other statistical parameter are listed in Tables 1 and 2. It is seen from the s that the values of  $\tau$  obtained by the model are not close to the experimental results. Thus, this model is not suitable for our case. This due to that the values of  $K_{YN}$  decrease with decreasing the flow rate, whereas, the corresponding values of  $\tau$  increased with increasing flow rate. A similar trend was followed for sorption of total hardness ( $\text{Ca}^{2+} + \text{Mg}^{2+}$ ) for zeolite- 4A column sorption (Razavi, McCoy et al. 1978).

**Table 2.** The values of Yoon and Nelson statistical parameter after removing total hardness ( $\text{Ca}^{2+} + \text{Mg}^{2+}$ ) by zeolite.

$\tau$	R 2	KYN	Flow ( $\text{mL min}^{-1}$ )
-585.62	0.8466	-7E-05	10
-152.57	0.9513	-0.0012	20
-57.829	0.9355	-0.0022	30

#### 4. CONCLUSION

The ground water sample that collected from Assiut Governorate wells were analyzed to determine the various physicochemical parameters such as TDS (Total Dissolved Solids), EC (Electrical Conductivity), Total Hardness ( $\text{Ca}^{2+}$ ,  $\text{Mg}^{2+}$ ) and total Alkalinity, the results reveals that physicochemical parameters are more than the desirable limit of WHO (World Health Organization) drinking water quality guideline. In this research, several synthetic zeolite 4A dose are selected and their efficiency as hardness removal from ground water were checked. The zeolite 4A synthesized was characterized using SEM, XRD. The packed bed investigation on the zeolite 4A revealed the importance of bed height, flow rate and inlet solute concentration on zeolite 4A. The column performance was better at higher inlet concentration, while the lowest flow rate and bed depth favored the column chemisorption. It's found that the efficiency of synthetic zeolite 4A on removal of total hardness removal ranged from 35% to

100% for  $\text{Ca}^{2+}$  and  $\text{Mg}^{2+}$ , respectively. The column data were well described using Thomas and Yoon–Nelson models. The Yoon–Nelson model was successfully used to predict the breakthrough curves at different flow rates and inlet MG concentrations.

#### ACKNOWLEDGMENTS

First of all my supervisors Prof. Dr. Abdel Hay Ali Farrag (Geology Department, Assiut University) and Prof. Dr. Thanaa Abdel Moghny. We appreciate the supporting offered by the research assistant Mahmoud Fathy Mubarak (Applications Department, Egyptian Petroleum Research Institute).

Special thanks to the Head of Assiut and new valley company for water and waste water Eng. Mohamed Salah El Deen Abdel Ghaffar for his supporting to our Team Research.

Finally, thanks to Ch. Esslam M. Hassanin, Ch. Zainab Fathy Mahmoud, Ch. Aliaa Mokhtar, Ch. Mariana Essmat and other my colleagues of the entire

Laboratories Sector staff of Assiut and new valley company for water and waste water for using the facilities of the Laboratories Tools.

## REFERENCES

1. Abanades, J. C., B. Arias, A. Lyngfelt, T. Mattisson, D. E. Wiley, H. Li, M. T. Ho, E. Mangano and S. Brandani (2015). "Emerging CO<sub>2</sub> capture systems." *International Journal of Greenhouse Gas Control* 40: 126-166.
2. Abd El Hay Ali Farrag, T. A. M., Atef Mohamed Gad Mohamed, Saleem Sayed Saleem, Mahmoud Fathy (2016). "Abu Zenima synthetic zeolite for removing iron and manganese from Assiut governorate groundwater, Egypt." *Applied Water Science*: DOI: 10.1007/s13201-13016-10435-y.
3. Ben Abda, M., O. Schäf and Y. Zerega (2015). "Ion exchange effect on asymmetric dioxins adsorption onto FAU-type X-zeolites." *Microporous and Mesoporous Materials* 217: 178-183.
4. Bertoni, F. A., A. C. Medeot, J. C. González, L. F. Sala and S. E. Bellú (2015). "Application of green seaweed biomass for MoVI sorption from contaminated waters. Kinetic, thermodynamic and continuous sorption studies." *Journal of Colloid and Interface Science* 446: 122-132.
5. Bhatia, S., A. Z. Abdullah and C. T. Wong (2009). "Adsorption of butyl acetate in air over silver-loaded Y and ZSM-5 zeolites: Experimental and modelling studies." *Journal of Hazardous Materials* 163(1): 73-81.
6. Cai, Q., B. D. Turner, D. Sheng and S. Sloan (2015). "The kinetics of fluoride sorption by zeolite: Effects of cadmium, barium and manganese." *Journal of Contaminant Hydrology* 177-178: 136-147.
7. Calvo, B., L. Canoira, F. Morante, J. M. Martínez-Bedia, C. Vinagre, J.-E. García-González, J. Elsen and R. Alcantara (2009). "Continuous elimination of Pb<sup>2+</sup>, Cu<sup>2+</sup>, Zn<sup>2+</sup>, H<sup>+</sup> and NH<sub>4</sub><sup>+</sup> from acidic waters by ionic exchange on natural zeolites." *Journal of Hazardous Materials* 166(2-3): 619-627.
8. Chen, H., H. Zhang and Y. Yan (2012). "Preparation and characterization of a novel gradient porous ZSM-5 zeolite membrane/PSSF composite and its application for toluene adsorption." *Chemical Engineering Journal* 209: 372-378.
9. Devrim, Y. and A. Albostan "Enhancement of PEM fuel cell performance at higher temperatures and lower humidities by high performance membrane electrode assembly based on Nafion/zeolite membrane." *International Journal of Hydrogen Energy*.
10. El Tahlawi, M. R., A. A. Farrag and S. S. Ahmed (2008). "Groundwater of Egypt: "an environmental overview"." *Environmental Geology* 55(3): 639-652.
11. Fathy, M., T. A. Moghny, A. E. A. Allah and A. Alblehy (2014). "Cation exchange resin nanocomposites based on multi-walled carbon nanotubes." *Applied Nanoscience* 4(1): 103-112.
12. Grande, C. A. and A. E. Rodrigues (2004). "Adsorption Kinetics of Propane and Propylene in Zeolite 4A." *Chemical Engineering Research and Design* 82(12): 1604-1612.
13. Guo, X., L. Zeng and X. Jin (2013). "Advanced regeneration and fixed-bed study of ammonium and potassium removal from anaerobic digested wastewater by natural zeolite." *Journal of Environmental Sciences* 25(5): 954-961.
14. Gupta, A., V. Gaur and N. Verma (2004). "Breakthrough analysis for adsorption of sulfur dioxide over zeolites." *Chemical Engineering and Processing: Process Intensification* 43(1): 9-22.
15. Han, R., L. Zou, X. Zhao, Y. Xu, F. Xu, Y. Li and Y. Wang (2009). "Characterization and properties of iron oxide-coated zeolite as adsorbent for removal of copper(II) from solution in fixed bed column." *Chemical Engineering Journal* 149(1-3): 123-131.
16. Hosseini, S. M., S. Rafiei, A. R. Hamidi, A. R. Moghadassi and S. S. Madaeni (2014). "Preparation and electrochemical characterization of mixed matrix heterogeneous cation exchange membranes filled with zeolite nanoparticles: Ionic transport property in desalination." *Desalination* 351: 138-144.
17. Inglezakis, V. J. and H. Grigoropoulou (2004). "Effects of operating conditions on the removal of heavy metals by zeolite in fixed bed reactors." *Journal of Hazardous Materials* 112(1-2): 37-43.
18. Kazemimoghadam, M. and T. Mohammadi (2007). "Synthesis of MFI zeolite membranes for water desalination." *Desalination* 206(1-3): 547-553.
19. Luukkonen, T., H. Runtti, M. Niskanen, E.-T. Tolonen, M. Sarkkinen, K. Kemppainen, J. Rämö and U. Lassi (2016). "Simultaneous removal of Ni(II), As(III), and Sb(III) from spiked mine effluent with metakaolin and blast-furnace-slag geopolymers." *Journal of Environmental Management* 166: 579-588.
20. M. El-Sayed, M. R., R. Hosny, M. Fathy, Th. Abdel Moghny (2016). "Breakthrough curves of oil adsorption on novel amorphous carbon thin film." *Water Science and Technology* 73 (10).

21. Mahmoud Fathy 1, Th. Abdel Moghny 1 , M. M. Abdou 1 , Abdel-Hameed A-A. El-Bellihi 2, and A. E. A. 1 (2015). "Study the Adsorption of Ca (II) and Mg (II) on High CrossLinked Polystyrene Divinyl Benzene Resin." *International Journal of Modern Chemistry* 7(1): 36-44.
22. Mahmoud Fathy, T. A. M., Mahmoud Ahmed Mousa, Abdel-Hameed A-A. El-Bellihi, Ahmed E. Awadallah (2016). "Absorption of calcium ions on oxidized graphene sheets and study its dynamic behavior by kinetic and isothermal models." *Applied Nanoscience*: DOI: 10.1007/s13204-13016-10537-13208.
23. Mahmoud Fathy, T. A. M., Mahmoud Ahmed Mousa, Abdel-Hameed A-A. El-Bellihi, Ahmed E. Awadallah (2016). "Synthesis of Transparent Amorphous Carbon Thin Films from Cellulose Powder in Rice Straw." *Arabian Journal for Science and Engineering*: DOI: 10.1007/s13369-13016-12273-13365.
24. Marcussen, L. (1982). "Comparison of experimental and predicted breakthrough curves for adiabatic adsorption in fixed bed." *Chemical Engineering Science* 37(2): 299-309.
25. Mustafa, Y. A. and M. J. Zaiter (2011). "Treatment of radioactive liquid waste (Co-60) by sorption on Zeolite Na-A prepared from Iraqi kaolin." *Journal of Hazardous Materials* 196: 228-233.
26. Padilha, C. E. d. A., C. A. d. A. Padilha, D. F. d. S. Souza, J. A. d. Oliveira, G. R. d. Macedo and E. S. d. Santos (2015). "Prediction of rhamnolipid breakthrough curves on activated carbon and Amberlite XAD-2 using Artificial Neural Network and Group Method Data Handling models." *Journal of Molecular Liquids* 206: 293-299.
27. Razavi, M. S., B. J. McCoy and R. G. Carbonell (1978). "Moment theory of breakthrough curves for fixed-bed adsorbers and reactors." *The Chemical Engineering Journal* 16(3): 211-222.